Dislocation-mediated healing of ideal and adsorbed monolayers with vacancy damage

B. Joós* and Z. Zhou†
Ottawa Carleton Institute of Physics, University of Ottawa Campus, Ottawa, Ontario, Canada K1N 6N5

M. S. Duesbery‡
Fairfax Materials Research Inc., 5613 Marble Arch Way, Alexandria, Virginia 22310-4011
(Received 28 April 1994)

A spontaneous self-healing mechanism, called dislocation-mediated healing (DMH), is demonstrated by molecular-dynamics simulation in ideal (i.e., constrained in two dimensions) and adsorbed monolayers. The self-healing involves a rapid condensation of the vacancies into dislocation dipoles. It is complete at temperatures above the self-diffusion temperature. An associated collapse of the shear modulus similar to the Kosterlitz-Thouless dipole dissociation is observed for high vacancy concentrations. The phenomenon is observed in monolayers with a long-range interparticle interaction and is more effective as the mobility of the vacancies increases. In Lennard-Jones monolayers (LJM's) a small compressive pressure is required to observe the effect. In a system with a longer-range potential it has been observed even with the monolayer under expansion. It also occurs in monolayers with nearest-neighbor piecewise-linear force interactions (PLFM's) under pressure provided that a third degree of freedom is present. But in general, in PLFM's vacancies agglomerate into clusters (voids). The same applies to LJM's below a critical pressure which decreases with temperature and vacancy concentration. The annealing of the vacancies by the formation of voids is a slower process than DMH, usually by at least an order of magnitude.

I. INTRODUCTION

Vacancies are the simplest and most common defects in any solid. They are particularly abundant in thin films, membranes, and surfaces where exchange with the environment and damage from external projectiles offer additional avenues for the creation of these defects. In physisorbed monolayers concentrations as high as 10 at. % before melting have been reported.[1] The logical questions are how a lattice sustains such a high vacancy concentration and whether at these concentrations the lattice is still an elastic medium. From another perspective it is intriguing to determine under what conditions the vacancy damage will repair itself in a two-dimensional system. This question has potentially a wide range of applications. In a protective coating, for instance, one form of lifetime-limiting damage is erosion by bombardment by atmospheric gases or space dust. Also, organic membranes and cells usually show self-repair tendencies and it is intriguing to investigate whether their intrinsic physical structure favors healing.

Recently we have shown[2] that, although vacancies are local defects, a concentration of just a few percent can have profound consequences on the macroscopic physical properties of a simple monolayer. Specifically we demonstrated, by a constant pressure molecular-dynamics (MD) simulation, a unique self-repair mechanism in an ideal (i.e., with in-plane degrees of freedom only) slightly compressed Lennard-Jones monolayer (LJM). The self-repair is associated with a shear modulus collapse similar to the melting scenario proposed in the Kosterlitz-Thouless-Halperin-Nelson-Young (KTHNY)[3] theory of two-dimensional melting. In this mechanism, which we could call dislocation-mediated healing (DMH), vacancies condense rapidly into dislocation dipoles, repairing the lattice; the dipoles then dissociate inducing an intermediate quasifluid state, leading eventually to the annealing of the defects at the edges. These effects occur for temperatures just above the self-diffusion temperature. In the present paper we give a more detailed discussion of the above results and investigate further the conditions which favor DMH, focusing notably on the effects of the range of the interparticle interaction, the pressure, and the third degree of freedom (in the direction normal to the plane of the monolayer).

The paper is organized as follows. The following section introduces the three model systems used in our simulations. Section III discusses the calculation of the elastic constants. In Secs. IV and V the results for the various ideal monolayers are presented, including a subsection on constant pressure versus constant volume simulations (Sec. IV C). In Sec. VI we present the effects of the third degree of freedom. We conclude in Sec. VII with a discussion.

II. THE MODEL SYSTEMS

Monolayers can appear in many forms with various interactions. We focus on monolayers formed of particles interacting with central forces. Two types of monolayers are considered in detail in this paper, one with a long-range interaction, the Lennard-Jones potential (LJP) monolayer (LJM), and the other held together by the nearest-neighbor piecewise linear force potential (PLFP), the piecewise linear force monolayer (PLFM). The self-healing mechanism discussed above is seen mainly in the

ideal LJM. The other system, the PLFM, exhibits very different behavior. It usually does not heal, but rather tends to develop voids. To explore further the effect of the range of the interacting potential, we also consider the monolayer with a 4-8 potential (4-8P) interaction, in short called the 4-8M. The reasons for choosing the 4-8P are that it is easy to compare it with the LJP and PLFP and that it has a longer range than either of the other two.

The LJP energy between two atoms at a distance r from each other is given by

$$V_{\mathrm{LJP}}(r)=4\epsilon\left[\left[\frac{\sigma}{r}\right]^{12}-\left[\frac{\sigma}{r}\right]^{6}\right]. \tag{1}$$

The cutoff of the LJP in our simulations was chosen to be $r=2.5\sigma$. The PLFP energy between two atoms at a distance r from each other is given by

$$V_{\mathrm{PLFP}}(r)=\begin{cases}\frac{1}{2}\kappa(r-d_0)^2-\kappa w^2\ , & r\le d_0+w\\ -\frac{1}{2}\kappa(r-d_0-2w)^2\ , & d_0+w<r\le d_0+2w\\ 0\ , & r>d_0+2w\ .\end{cases} \tag{2}$$

w is taken to be $0.15d_0$, as in Ref. 4. For this value of w the dislocation core has only one broken bond. Smaller values of w lead to more broken bonds in the core. The 4-8P is given by

$$V_{4-8}(r)=4\epsilon'\left[\left[\frac{\sigma'}{r}\right]^{8}-\left[\frac{\sigma'}{r}\right]^{4}\right], \tag{3}$$

with a cutoff at $r=(2.5)^{1.5}\sigma'=5.196\sigma'$.

Monolayers formed of particles interacting with central forces will tend to form triangular lattices. This is the closest packing in two dimensions and it is favored at densities where the nearest-neighbor interparticle distance is close to the minimum of the interparticle interaction. That is the case whenever the pressure is not too large, as is the case in our situations. Lattices with fewer nearest neighbors are obtained at very high pressure.[5]

The LJM and PLFM have been extensively studied, although the motivations of the studies were different. The PLFM has been used mostly in simulations of the plasticity of solids[4,6] whereas the LJM was used extensively in attempts to understand the nature of the melting transition in two dimensions (for reviews see Refs. 7 and 8). Recently the melting behavior of the PLFM was also considered.[9] Usually the role of the vacancies in the change of the elastic properties has been ignored. This paper attempts to assess their significance. The fact that one potential is very short range (PLFP) and the others relatively long range (LJP and 4-8P) will allow us to determine whether vacancy related properties are significantly altered by the range of the interacting potential. We also considered the effects of the substrate by applying a smooth (without corrugation) holding potential to the LJM and the PLFM. The potential chosen is the type occurring in physisorption and is of the van der Waals type. It was first calculated by Steele[10] for a graphite structure and his potential is given by

$$V_{\mathrm{sub}}(z)=\frac{4\pi\epsilon\sigma^6}{a_s d^4}\left[\frac{2}{5}\left[\frac{\sigma}{d}\right]^6\left[\frac{z}{d}\right]^{-10}-\left[\frac{z}{d}\right]^{-4}-\frac{1}{3}\left[\frac{z}{d}+0.61\right]^{-3}\right], \tag{4}$$

where a_s is the area of the basal-plane unit cell and d the interlayer spacing. It can be rewritten in reduced units as

$$V_{\mathrm{sub}}(z)=a_0[a_1 z^{-10}-a_2 z^{-4}-\tfrac{1}{3}(a_3 z+0.61)^{-3}]\ . \tag{5}$$

a_0 can be used as a measure of the strength of the holding potential. In our simulation, we took $a_1=0.1230$, $a_2=0.6148$, and $a_3=1.1293$. These would be the values for Xe adsorbed on graphite. Several values of a_0 were considered, $a_0=0.4\kappa d_0^2$, $0.3\kappa d_0^2$, and $0.03\kappa d_0^2$. The largest value applies to Xe on graphite but, as we shall see, for that value the potential is already strong enough to prevent any significant change from the ideal monolayer case. Most calculations were done for $a_0=0.3\kappa d_0^2$, which gives a depth of the holding potential of about $V_{\mathrm{sub}}(0.8855)=-0.1995\kappa d_0^2$.

We first performed simulations at constant pressure and constant temperature with periodic boundary conditions (PBC). The damped force method was used to keep the temperature constant and the Andersen method for maintaining the pressure constant.[11] To investigate the dependence of our results on the choice of the ensemble we also performed some constant-volume and constant-temperature simulations.

The three potentials have been chosen to have the same depth, equal to κw^2, and the same minimum ($\sigma=2^{-1/6}d_0$ and $\sigma'=2^{-1/4}d_0$). For the PLFP the depth is set by the value of w which has been taken as $0.15d_0$; consequently for the LJP and the 4-8 potential $\epsilon=\epsilon'=0.0225\kappa d_0^2$. The basic time step is $0.1t_0$, where t_0 is the unit of time $\sqrt{m/\kappa}$. Unless otherwise mentioned our samples are rhombuses with 28 atoms on the side. Some simulations were done on rhombuses with 51 atoms on the side to see if there are any qualitative size effects.

III. CALCULATION OF THE ELASTIC CONSTANTS

Elastic constants yield valuable dynamical and mechanical information about the effect of the vacancies on the monolayer. For example, they yield information concerning the stability or strength of the system and can be used as order parameters to monitor the healing process. In a continuum theory vacancies have no effect on the elastic properties of a system of particles. Consequently the effects we will be discussing in this paper are beyond the predictions of continuum elasticity theory.

At zero temperature the calculation of elastic constants follows the arguments first given by Born and Huang[12] and also found in Ref. 13. The elastic constants are obtained from the long-wavelength limit of the elastic waves.

To obtain an expression for the elastic constants which is valid at finite temperatures, an approach different from the one used at zero temperature is necessary. Squire, Holt, and Hoover[14] showed in 1969 that expressions in

the canonical ensemble (which implies constant volume) can be easily derived from the Helmholtz free energy $\Omega=E-TS=-k_BT\ln Z$, where k_B is the Boltzmann constant and Z the classical partition function for the crystal. Z is a relatively simple sum over all configurational energies:

$$Z=\frac{1}{N!\hbar^{3N}}\int e^{-\mathbf{H}/k_BT}d\tau\ , \tag{6}$$

where $d\tau$ is the differential volume element in $(6N)$-dimensional phase space and

$$\mathbf{H}=\sum_i\frac{\vec{p}_i^{\,2}}{2m}+\sum_{i>j}\phi(\vec{r}_{ij})\ . \tag{7}$$

Using the second law of thermodynamics (see, for instance, Ref. 15),

$$TdS=dE+V_0\mathrm{Tr}(td\epsilon)\ , \tag{8}$$

where V_0 is the volume of the unstrained system, t is the internal thermodynamic tension tensor, and ϵ is the macroscopic strain tensor, we find

$$d\Omega=-SdT-V_0\sum_{\alpha\beta}t_{\alpha\beta}d\epsilon_{\beta\alpha}\ . \tag{9}$$

From (9) we obtain the following

$$t_{\alpha\beta}=-\frac{1}{V_0}\left[\frac{\partial\Omega}{\partial\epsilon_{\alpha\beta}}\right]_T\ , \tag{10}$$

$$C_{\alpha\beta\gamma\delta}=-\left[\frac{\partial t_{\alpha\beta}}{\partial\epsilon_{\gamma\delta}}\right]_T=-\frac{1}{V_0}\left[\frac{\partial^2\Omega}{\partial\epsilon_{\alpha\beta}\partial\epsilon_{\gamma\delta}}\right]_T\ . \tag{11}$$

For an isotropic solid such as the two-dimensional triangular lattice, there are only two independent elastic constants. Traditionally $\lambda=C_{1122}=C_{12}$ and $\mu=C_{1212}=C_{44}$ are chosen to characterize the system. Using Eq. (11) these constants can be written as

$$\lambda=\frac{1}{Ak_BT}\left\{\left\langle\sum\frac{\phi'}{r}(\Delta x)^2\right\rangle\left\langle\sum\frac{\phi'}{r}(\Delta y)^2\right\rangle-\left\langle\sum\frac{\phi'}{r}(\Delta x)^2\otimes\sum\frac{\phi'}{r}(\Delta y)^2\right\rangle\right\}+\frac{1}{A}\left\langle\sum\frac{\phi''}{r^2}(\Delta x)^2(\Delta y)^2\right\rangle$$
$$-\frac{1}{A}\left\langle\sum\frac{\phi'}{r^3}(\Delta x)^2(\Delta y)^2\right\rangle-\frac{1}{A}\left\langle\sum\frac{\phi'}{r}(\Delta x)^2\right\rangle\ , \tag{12}$$

$$\mu=\frac{1}{Ak_BT}\left\{\left\langle\sum\frac{\phi'}{r}\Delta x\Delta y\right\rangle^2-\left\langle\left[\sum\frac{\phi'}{r}\Delta x\Delta y\right]^2\right\rangle\right\}+\frac{1}{A}\left\langle\sum\frac{\phi''}{r^2}(\Delta x)^2(\Delta y)^2\right\rangle-\frac{1}{A}\left\langle\sum\frac{\phi'}{r^3}(\Delta x)^2(\Delta y)^2\right\rangle$$
$$+\frac{1}{A}\left\langle\sum\frac{\phi'}{r}(\Delta x)^2\right\rangle+\frac{Nk_BT}{A}\ , \tag{13}$$

where the quantities Δx and Δy represent the x and y coordinates of $\vec{r}_{ij}=\vec{r}_i-\vec{r}_j$, r the modulus of that vector, and A the area of the system. The sums are over all pairs of particles. The last thermal average in each equation is required when an external pressure is exerted on the solid. It arises from the term in the free energy which guarantees equilibrium with respect to volume change (for details see Ref. 16). The last term in Eq. (13) is the kinetic-energy contribution.

The above formulas have been used in Monte Carlo simulations. They are also applicable to constant-volume MD simulations. For an ensemble in which the angles of the MD cell vector and the diagonal thermodynamic tension is kept constant but the size of the system can fluctuate (for instance, see Ref. 17), the expression for μ can be shown to be still applicable.

For uniform dilation, such as in Andersen's ensemble,[11] the conserved thermodynamic potential is basically Gibb's potential and can be written as[18]

$$\mathbf{A}=E-TS+P(V-V_0)=E-TS+V_0\sum_\alpha t_{\alpha\alpha}\epsilon_{\alpha\alpha}\ , \tag{14}$$

since in this case the macroscopic strain tensor $\epsilon_{\alpha\alpha}$ and the thermodynamic stress tensor $t_{\alpha\alpha}$ are scalars: $3\epsilon_{\alpha\alpha}V_0=(V-V_0)$ and $t_{\alpha\alpha}=P$, where P is the internal hydrostatic pressure.

From Eq. (8) we obtain

$$d\,\mathbf{A}=-SdT-V_0\sum_\alpha\epsilon_{\alpha\alpha}dt_{\alpha\alpha}-V_0\sum_{\alpha\neq\beta}t_{\alpha\beta}d\epsilon_{\beta\alpha}\ , \tag{15}$$

from which it follows that

$$t_{\alpha\beta}=-\frac{1}{V_0}\left[\frac{\partial\,\mathbf{A}}{\partial\epsilon_{\alpha\beta}}\right]_{T,t_{\alpha\alpha}}\ , \tag{16}$$

$$C_{\alpha\beta\gamma\delta}=\left[\frac{\partial t_{\alpha\beta}}{\partial\epsilon_{\gamma\delta}}\right]_{T,t_{\alpha\alpha}}=-\frac{1}{V_0}\left[\frac{\partial^2\,\mathbf{A}}{\partial\epsilon_{\alpha\beta}\partial\epsilon_{\gamma\delta}}\right]_{T,t_{\alpha\alpha}} \tag{17}$$

for $i\neq j$ and $k\neq l$. Only off-diagonal elastic constants, such as the shear modulus, are accessible from this thermodynamic potential.

The fundamental connection between thermodynamics and statistical mechanics gives

$$\mathbf{A}=-k_BT\ln\Theta\ , \tag{18}$$

where

$$\Theta=\frac{1}{N!\hbar^{3N}}\int e^{-\mathbf{H}/k_BT}d\tau\,d\epsilon_{11}d\epsilon_{22}d\epsilon_{33} \tag{19}$$

and

$$\mathbf{H}=\sum_i \frac{\vec{p}_i^{\,2}}{2m}+\sum_{i>j}\phi(\vec{r}_{ij})+V_0\sum_\alpha t_{\alpha\alpha}\epsilon_{\alpha\alpha} . \quad (20)$$

Because of the integration in Θ over the diagonal elements of the strain, the formulas for the off-diagonal elastic constants are the same as in the canonical ensemble, i.e., Eq. (13) still applies. In the present work, Eq. (13) was used to calculate μ in both the constant-pressure and constant-area ensembles and the results were found to be consistent (see Sec. IV C).

Diagonal elements of $C_{\alpha\beta\gamma\delta}$ cannot be obtained from Eq. (17) as is evident from Eq. (15), but they have to be expressed in terms of fluctuations in the strain[19,20] as

$$\frac{k_B T}{V}(C^{-1})_{\alpha\beta\gamma\delta}=\delta(\epsilon_{\alpha\beta}\epsilon_{\gamma\delta}) . \quad (21)$$

But as pointed out by Sprik, Impey, and Klein[21] and others,[22,18] the rate of convergence of Eq. (21) is unsatisfactory. It is much more efficient to first determine the equilibrium lattice constant for the pressure of interest using a constant pressure simulation and then do a simulation in the corresponding canonical (constant volume) ensemble[22] using formulas obtained from Eq. (11), i.e., in our case Eqs. (12) and (13). This can be understood if one observes that Eq. (21) follows the fluctuations in a macroscopic quantity which evolves slowly, especially in a large system. In contrast Eqs. (12) and (13) calculate the elastic constants by probing microscopic features of the system where fluctuations occur on a shorter time scale.

Elastic properties for the two-dimensional LJM do not seem to be available in print even for zero temperature. Values are, however, reported for some rare-gas solids[23] which are very close to the LJM. In contrast, simple analytical results can be derived for the PLFM at zero temperature. For this case the Lamé parameters are given by

$$\mu=(\sqrt{3}/4)(4-3\rho^{1/2})\kappa , \quad (22)$$

$$\lambda=(\sqrt{3}/4)(5\rho^{1/2}-4)\kappa , \quad (23)$$

where ρ is the density relative to the equilibrium.[6]

Using the formula for the contribution of the interparticle interactions to the pressure,

$$P=\frac{1}{2A}\sum_{i<j}\vec{F}_{ij}\cdot\vec{r}_{ij} , \quad (24)$$

where $\vec{F}_{ij}$ and $\vec{r}_{ij}$ are, respectively, the force of interaction and the vector joining particles i and j, it is straightforward to show that, in the perfect PLFM with only nearest-neighbor interactions, at zero temperature the pressure P is related to the lattice constant d by

$$P=\sqrt{3}\left[\frac{d_0}{d}-1\right]\kappa . \quad (25)$$

Using this equation, the elastic constants can be rewritten in terms of P:

$$\mu=(\sqrt{3}/4)\left[1-\sqrt{3}\frac{P}{\kappa}\right]\kappa , \quad (26)$$

$$\lambda=(\sqrt{3}/4)\left[1+\frac{5P}{\sqrt{3}\kappa}\right]\kappa . \quad (27)$$

Hence the zero-temperature elastic constants for a perfect PLFM at a pressure of 0.0053κ are $\lambda=0.446\kappa$ and $\mu=0.425\kappa$, varying little for a large range of pressures. In contrast, for the LJM with $P=0.0087\kappa$, $\lambda=0.836\kappa$ and $\mu=0.825\kappa$. The LJM, because of its longer range interactions, is a stiffer solid.

IV. RESULTS FOR THE IDEAL LJM AND PLFM

First, we consider the ideal monolayer which has only in-plane degrees of freedom. Some preliminary results on the slightly compressed LJM and PLFM have been reported earlier.[2] For the range of pressure of interest, the melting temperature is about the same in both systems, specifically $0.010\kappa d_0^2/k_B$ for the LJM (Refs. 24 and 7) and $0.011\kappa d_0^2/k_B$ for the PLFM.[9] In comparison the self-diffusion temperature for vacancies T_D in these systems is approximately $0.0055\pm0.0005\kappa d_0^2/k_B$.

A. Low-temperature elastic constants (below T_D)

At temperatures below T_D, the vacancies do not move over long time intervals. The elastic constants measure the weakening of the system in the presence of the defects. Figure 1 shows the variation, as a function of vacancy concentration c_n, of the shear modulus (μ) and the bulk modulus ($B=\lambda+\mu$), normalized to their respective perfect lattice values μ_0 and B_0. The temperature was $T=0.002\kappa d_0^2/k_B$ and vacancy concentrations from 0 to 3.8 at. % were considered. The pressure on the LJM was 0.0087κ while on the PLFM it was 0.0053κ.

The range of the potential seems to have little effect on the rate of decrease of the shear or bulk modulus with increasing vacancy concentration. The shear modulus loses a fifth of its value for a 4 at. % concentration

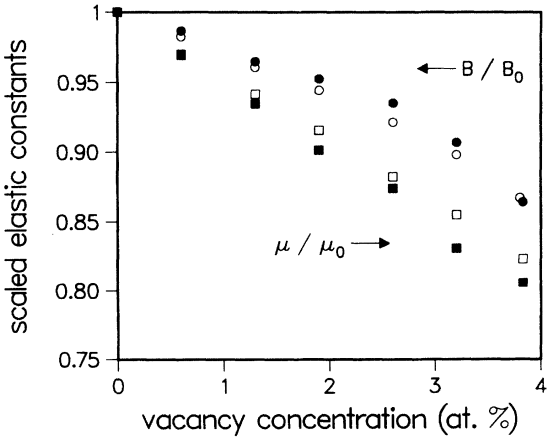

FIG. 1. Variation of the shear modulus μ (squares) and the bulk modulus $B=\lambda+\mu$ (circles), both normalized to the zero vacancy values μ_0 and B_0, respectively, as a function of vacancy concentration for the LJM (full symbols) and the PLFM (open symbols) at the temperature $0.002\kappa d_0^2/k_B$.

of vacancies. This corresponds to $\Delta\mu/\mu_0=(\mu-\mu_0)/\mu_0=-5c_n$. The bulk modulus decreases at the slightly lower rate $\Delta B/B_0\simeq-3.5c_n$. As Fig. 1 shows, there is a scatter in the data with vacancies present. For each concentration there are many possible configurations of vacancies. Figure 1 shows the average over several configurations for each concentration.

B. Self-repair mechanisms (above T_D)

As the temperature is raised, the vacancies start to move. Two types of behavior, which are illustrated in Fig. 2, are observed above the diffusion temperature. Either the vacancies condense rapidly into a dislocation dipole, what we call dislocation-mediated healing (DMH)

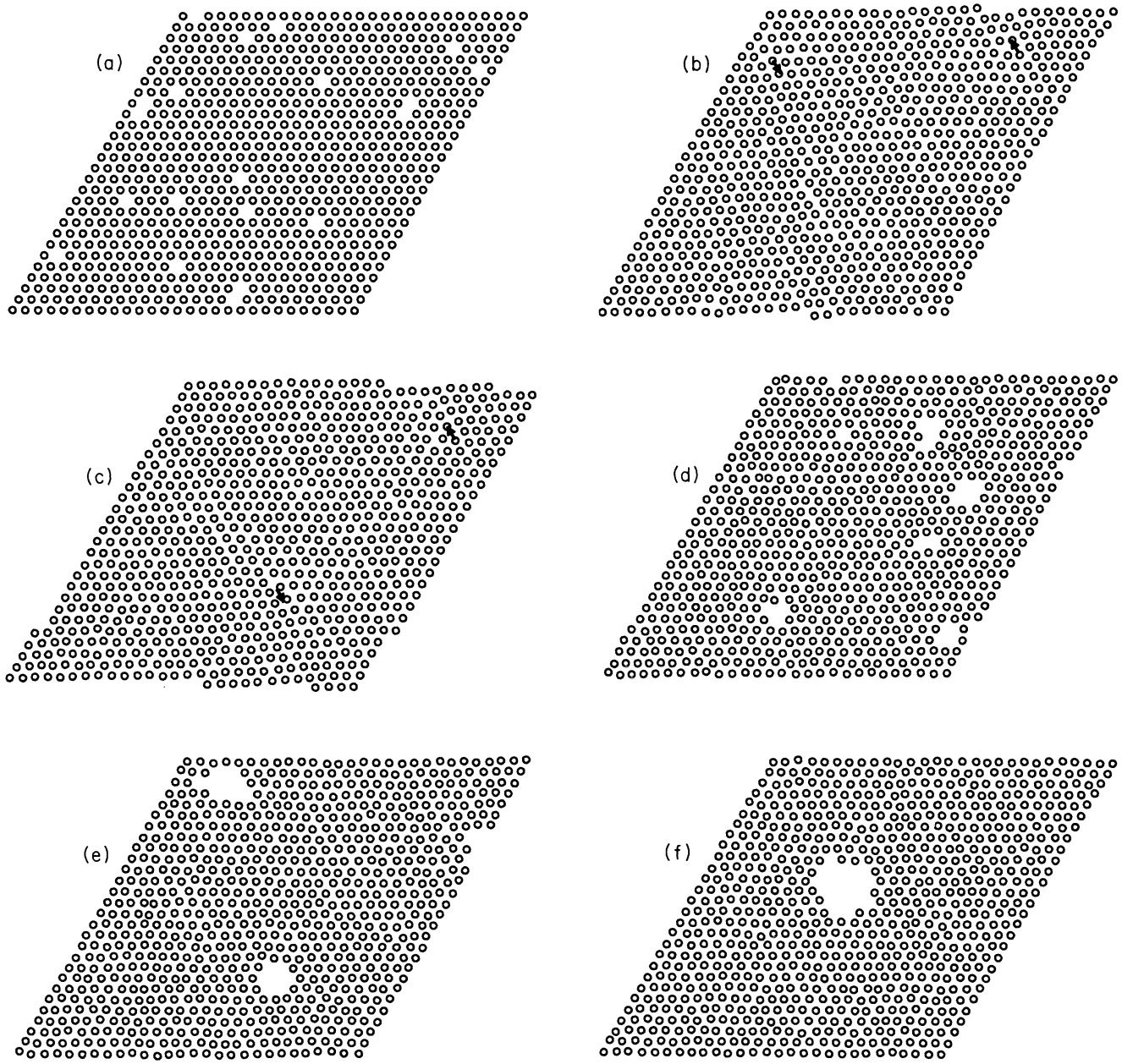

FIG. 2. (a) Typical low-temperature configuration of atoms for either the LJM or the PLFM for a vacancy concentration of $c_n=2.56$ at. %. (b) and (c) Same configuration after relaxation during a time $t=46\,000t_0$ and $56\,500t_0$, respectively, at the temperature $T=0.006\kappa d_0^2/k_B$ in the LJM with pressure 0.087κ (the arrows placed at the cores of the dislocations are Burgers vectors). This is an example of dislocation-mediated healing. In (b) we have a 60° dipole with the burgers vector making an angle of 60° with the vector joining the two dislocations. The vacancies are lines up in a row. In (c) the dislocations have glided along the direction of their burgers vector. (d)–(f) started with the same initial configuration (a), but are for the PLFM at the same temperature as the LJM, but with pressure $P=0.0053\kappa$. They show the different stages of the formation of a large void: (d) at $t=360\,000t_0$, (e) at $t=1\,118\,000t_0$, and (f) at $t=1\,850\,000t_0$.

[Figs. 2(b) and 2(c)], or they diffuse slowly into small vacancy clusters [Fig. 2(d)], which eventually anneal out of the system by forming a large void [Figs. 2(e) and 2(f)].

1. *The Lennard-Jones monolayer*

In the LJM, under slight pressure (specifically 0.0087κ in the runs below) the first scenario occurs when the vacancies are in sufficient number. For fewer than 15 vacancies in a rhombus 28 atoms on the side (or $c_n < 1.9$ at. %), the vacancies diffuse into small vacancy clusters. For 15 vacancies or more (or $c_n \geq 1.9$ at. %), the vacancies are removed by condensing into a "large" vacancy dislocation dipole (separation equal to larger than 15 atomic rows) [see Fig. 2(b)].[23,25] The PBC introduce a periodicity in the behavior of our system [see Fig. 3(a)]. For more than 28 vacancies (or $c_n > 3.6$ at. %) there are more vacancies than would fit into one dipole, so 28 vacancies are annealed out and the remainder form vacancy clusters unless their numbers exceed the minimum required to form a second large dipole. When a dipole is present in the sample, the shear modulus collapses [see Fig. 3(a)]. The dipole appears very quickly, within a few thousand t_0 or a few nanoseconds if parameters appropriate to Xe are used. To complete the process, which means that the average lattice constant and the shear modulus have stabilized, takes longer, about $30\,000t_0$ (or about 20 ns with Xe parameters). This is an upper limit obtained with vacancies uniformly placed on the sample. With other configurations the times were shorter.

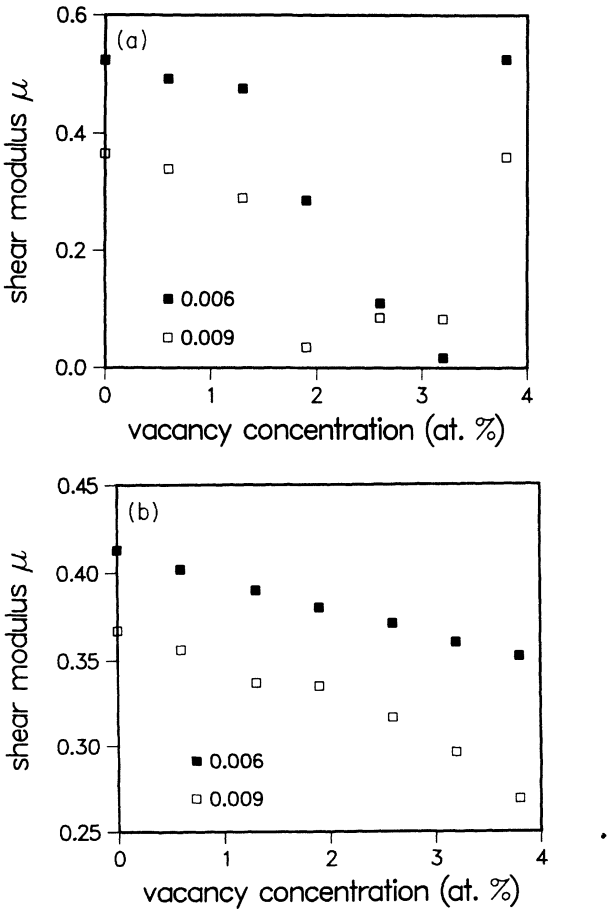

FIG. 3. Variation of the shear modulus (in units of κ) as a function of vacancy concentration for temperatures of $0.006\kappa d_0^2/k_B$ and $0.009\kappa d_0^2/k_B$ for (a) the LJM (at a pressure $P=0.0087\kappa$) and (b) the PLFM ($P=0.0053\kappa$).

The above behavior, which we call dislocation-mediated healing, is consistent with our findings on the properties of dislocation dipoles in LJP-type monolayers.[23,25–27] In these references it is shown that dipoles containing less than 15 vacancies (or $c_n < 1.9$ at. %) behave more like composite pinned defects than elastic dipoles. They are the favored defects at very low vacancy concentrations. On the other hand, a logarithmic dependence of the energy on size makes large dipoles favorable at higher concentrations. These move nearly freely in the direction of their Burgers vector over a wide range of angles (45°–135°).[26,27] The high mobility of the dislocations leads to a loss of shear strength and translational order. One dipole is sufficient, although the effect may be enhanced by the screening resulting from similar dipoles (in our case in the neighboring cells of our periodic structure). The collapse in the shear modulus is similar to what occurs in the melting mechanism proposed by the KTHNY (Ref. 3) theory of two-dimensional melting, where dislocation dipoles are thermally activated, and under the action of their mutual screening dissociate, leading to a collapse of the shear modulus without loss of the bond orientational order.

DMH is observed for all pressures larger than a critical value 0.0066κ for $T=0.006\kappa d_0^2/k_B$, a temperature just slightly above the diffusion temperature T_D. For smaller pressures void formation is observed. In a typical run the annealing by the formation of a large void occurred within $100\,000t_0$, slower than DMH. In Fig. 4 we have

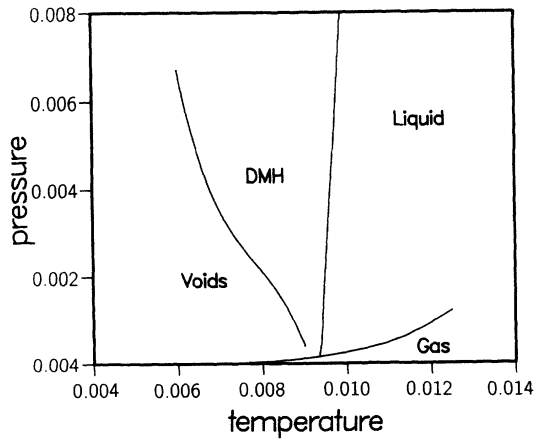

FIG. 4. Pressure versus temperature phase diagram of the LJM showing regions of dislocation-mediated healing and void formation in the solid phase for a vacancy concentration $c_n=0.0256$ at. %. The liquid, solid, and gas phase boundaries are Monte Carlo results of Barker, Henderson, and Abraham (Ref. 24). (Pressures in units of κ and temperatures in units of $\kappa d_0^2/k_B$. To convert pressures to ϵ/σ^2 and temperatures to ϵ/k_B multiply by 35.28 and 44.44, respectively.)

mapped out a phase diagram of the LJM showing in the solid phase the regions of DMH and void formation for a vacancy concentration $c_n=0.0256$ at.%. The line separating regions of DMH and void formation is a function of c_n, moving towards lower pressures with increasing c_n. When the temperature is raised DMH is more rapid and persists to lower pressures. Below $T_D\sim 0.0055\kappa d_0^2/k_B$ vacancy diffusion is very slow and the self-diffusion temperature is a natural boundary for DMH. Going to high temperatures the critical line goes to zero as the temperature approaches the tricritical point located at $T=0.009\,34\kappa d_0^2/k_B$ close to the zero pressure line.[24]

With the increase of the temperature towards the melting line the shear modulus collapse is more complete and occurs at lower vacancy concentrations. This can be seen in Fig. 3(a) for $P=0.0087\kappa$. It should be noted that the liquid-solid phase boundary is for zero-vacancy concentration. In this paper we restrict ourselves to the solid phase. The question of healing in the liquid phase opens up a new range of issues, which will not be addressed in this paper.

The preference for void formation at low pressure can be understood if one notes that as the pressure is decreased and can even become negative, the energies of the vacancy and the short dislocation dipoles drop rapidly,[25] making these defects and associated small defect clusters very favorable. These in turn then act as nuclei for a larger void.

2. *The piecewise linear force monolayer*

Void formation is the usual response of the short-range potential system, the PLFM, under vacancy damage. The vacancies form clusters which eventually combine into large voids [see Figs. 2(d) and 2(f)]. This typically takes much longer than DMH or even void formation in the LJM (at least by an order of magnitude). The precise time depends on the distribution of the vacancies. In the example shown in Fig. 2(f), it was as high as $1.85\times 10^6 t_0$ at $T=0.006\kappa d_0^2/k_B$ with a pressure of 0.0053κ. The PLFP is nearest neighbor, so as soon as a triangle of vacancies is formed, additional vacancies in the cluster do not add to the energy. In effect, one has a free surface and the vacancies anneal out, but remain within the system. The temperature-induced diffusion smooths out the elastic constants even before the voids are formed [see Fig. 3(b)]. There is no collapse of the shear modulus, which is reduced only by an amount comparable to the reduction in density. In this system vacancy clusters have lower energies than vacancy dislocation dipoles in contrast to those in the LJM.[27]

We have also considered pressures of 0.01κ and 0.02κ for $c_n=0.0256$ at.% at a temperature of $0.006\kappa d_0^2/k_B$ and still find no DMH. A larger sample size is not expected to make any difference either. A sample of 51×51 atoms for $c_n=2.56$ at.% showed the same cavitation behavior.

Zero and negative pressures were also considered with similar results. While the system under negative pressure expanded, the zero-pressure system contracted. This latter behavior is a peculiarity of the PLFM. The absence of a hard core in the PLFP favors interstitial types of defects at finite temperature.[27]

TABLE I. The shear moduli in constant-volume (μ_v) and constant-pressure (μ_p) ensembles for the LJM system at $T=0.006\kappa d_0^2/k_B$ with $P=0.0087\kappa$.

c_n	μ_v	μ_p
0.0000	0.490	0.498
0.0064	0.465	0.472
0.0130	0.450	0.446
0.0193	0.281	0.286

C. Constant pressure vs constant volume

The work described above was done in the constant-pressure and the constant-temperature ensemble with PBC. To check whether the choice of the ensemble has any influence on the behavior of the two systems we performed simulations in the constant-volume and constant-temperature ensemble for both the compressed LJM and PLFM with PBC. To avoid biasing the results, we did not use the output data (velocities, coordinates, etc.) of the constant-pressure runs as the input data of the constant-volume run. We started with samples of areas equal to the average area of a constant pressure run with the same number of vacancies after the initial compression which usually only takes about $2000t_0$. This means that there is a slight overcompression in the constant volume compared with the corresponding constant-pressure run. The same behavior is observed as in the constant pressure runs for the LJM and PLFM, but things happen over a longer time scale. It appears that volume fluctuations in the constant-pressure run favor large-scale readjustments of the particles and hence accelerate the healing.

Just to emphasize how similar the behavior in the two ensembles are, we show the shear moduli calculated in the constant-volume simulation. As can be seen from Tables I and II they are very close to those obtained in the constant-pressure runs at the same temperature and average pressure.

V. MONOLAYER WITH THE 4-8 INTERACTION POTENTIAL

Suspecting that the difference in behavior observed in the LJM and the PLFM was due to the longer range of the LJP with its ensuing consequences on vacancy in-

TABLE II. The shear moduli in constant-volume (μ_v) and constant-pressure (μ_p) ensembles for the PLFM system at $T=0.006\kappa d_0^2/k_B$ with $P=0.0053\kappa$.

c_n	μ_v	μ_p
0.0000	0.419	0.419
0.0256	0.370	0.370

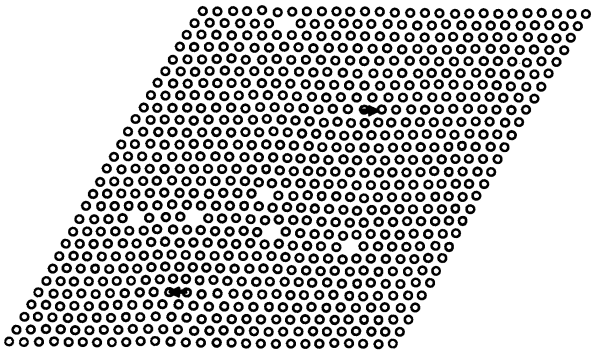

FIG. 5. Configurations of atoms of the system with the 4-8 interaction potential at $T=0.0015\kappa d_0^2/k_B$ and $c_n=2.56$ at. %, at pressure -0.0087κ and at $t=20\,000t_0$ and $d=0.9517d_0$.

teractions and dislocation properties, we considered a monolayer with an even longer-range interaction than the LJP, the 4-8P defined in Eq. (3). This system, the 4-8M, was found to exhibit DMH at all pressures considered, from $P=0.0087\kappa$ down to -0.0087κ, i.e., a DMH is preferred over the formation of voids *even at negative pressures.* At zero pressure the melting temperature is $0.0095\kappa d_0^2/k_B$ and the self-diffusion temperature $0.0036\pm0.0005\kappa d_0^2/k_B$. Typically a vacancy concentration of $c_n=2.56$ at. % was chosen. The DMH was found to be rapid also at zero pressure with a completion time of $\sim 30\,000t_0$ at $T=0.006\kappa d_0^2/k_B$, a fairly large temperature in this system. With negative pressure the DMH still appears quickly, but its completion time is very sensitive to temperature. With $P=-0.0087\kappa$ and $T=0.0045\kappa d_0^2/k_B$ the lattice parameter stabilizes after $20\,000t_0$, but after $450\,000t_0$, the lattice is still partially disordered when $T=0.006\kappa d_0^2/k_B$.

Contrary to the other two systems with a shorter-range potential, partial DMH was observed in the 4-8M below the isolated vacancy diffusion temperature, specifically at $T=0.0025\kappa d_0^2/k_B$ and $0.0015\kappa d_0^2/k_B$. The healing is not complete. As seen in Fig. 5, isolated vacancies remain in the system.

VI. EFFECT OF THE THIRD DEGREE OF FREEDOM

So far we have only considered the ideal monolayer, which is constrained to a two-dimensional space. In a real adsorbed system there is, however, always the third degree of freedom. The monolayer will be held by a holding potential, which can be weak or strong, and may or may not have significant lateral variations. We will not consider here the effects of the lateral variations. The third degree of freedom opens up new trajectories to the particles and, if the holding potential is not too strong, we can expect to find some qualitative changes in the healing mechanisms.

To study the changes brought about by the third degree of freedom, we applied a smooth (unmodulating) holding potential to both the LJM and the PLFM at the temperature $0.006\kappa d_0^2/k_B$. We found the behaviors sensitive to the pressure and the strength of the holding potential.

A. PLFM

For a very weak holding potential, the adsorbed atoms form rapidly a multilayer film instead of a monolayer. This is what is shown in Fig. 6(a) where a_0, the measure of the strength of the holding potential [see Eq. (5)], is equal to $0.03\kappa d_0^2$, $c_n=1.3$ at. %, the pressure is 0.0053κ, and the configuration is for a time $t=2000t_0$.

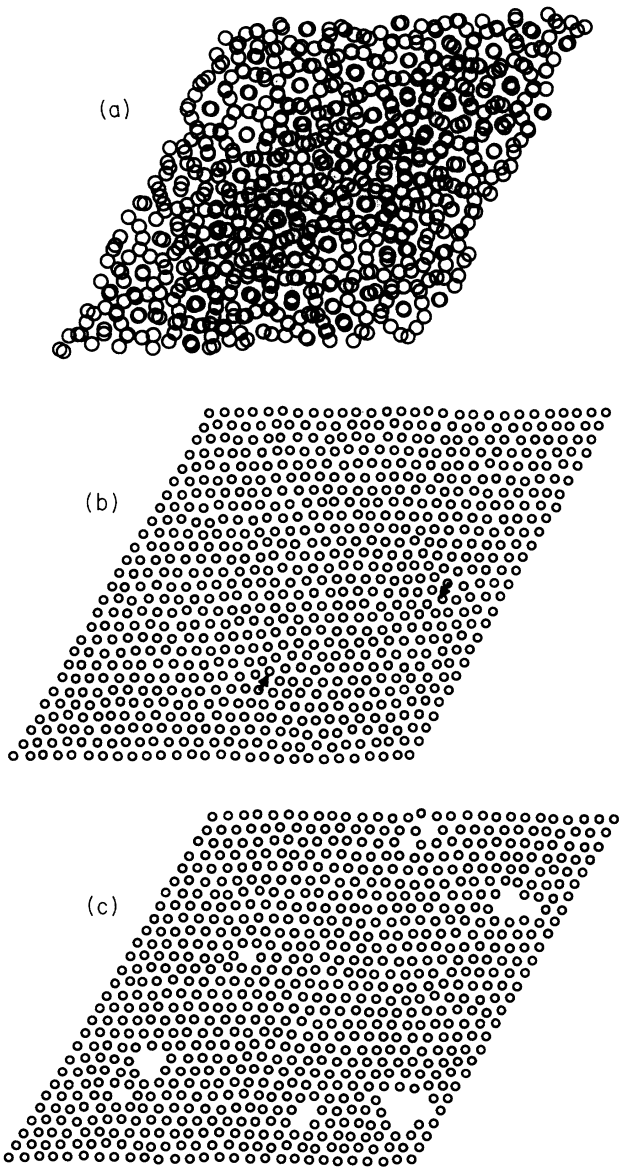

FIG. 6. Configurations of atoms for the PLFM with a smooth holding potential at $T=0.006\kappa d_0^2/k_B$ for several values of a_0, the strength of the holding potential: (a) $a_0=0.03\kappa d_0^2$, $c_n=1.3$ at. %, pressure 0.0053κ, and at $t=2000t_0$; (b) $a_0=0.3\kappa d_0^2$, $c_n=2.5$ at. %, pressure 0.0053κ, and at $t=167\,000t_0$ and $d=0.9814d_0$. (c) The same as (b), but the pressure is 0.0035κ, and $t=535\,000t_0$ and $d=0.9957d_0$.

In contrast, with a strong holding potential (such as with $a_0=0.4\kappa d_0^2$) the behavior of the system is similar to that of the ideal monolayer.

For an intermediate strength of the holding potential, something interesting happens. Though the interparticle interaction is short range, we find that the system will exhibit DMH with $a_0=0.3\kappa d_0^2$, $c_n=2.5$ at. %, and pressure equal to 0.0053κ. Figure 6(b) shows configurations with these conditions at time $167\,000t_0$. Similar to the ideal compressed monolayer, the vacancies are removed to condense into a large vacancy dislocation dipoles.

However, as we have found in the ideal monolayer, when the pressure becomes very low, the system shows no DMH. Cavitation is, however, quite slow. For a lateral pressure of 0.002κ, after $535\,000t_0$, as seen in Fig. 6(c), the voids are still fairly small and show no haste in condensing into a larger cavity. (The same applies for a pressure of 0.0035κ.)

B. LJM

At the intermediate strength of the holding potential $a_0=0.3\kappa d_0^2$, DMH is still observed in the LJM, and remains pressure dependent. At pressures below 0.0095κ voids are formed. But the time needed to form a large void is still considerably less than in the PLFM. For $P=0.0095\kappa$, a completed DMH was observed within $20\,000t_0$. For $P=0.0087\kappa$ a single large void was formed within less than $100\,000t_0$.

VII. CONCLUSIONS

In summary, just above the self-diffusion temperature and well below the melting temperature, only a very low concentration of isolated vacancies can be sustained in an ideal monolayer. What happens to the vacancies depends strongly on the range of the interparticle interaction. A short-range interaction favors the formation of voids, which can eventually combine to form a large cavity. When there is a sufficient number of vacancies, monolayers with long-range interparticle interactions heal through the creation of a dislocation dipole and an intermediate disordered state is formed, a process that we call dislocation-mediated healing. For the system with the 4-8P, the DMH remains rapid at zero pressure and still occurs, albeit slowly, at negative pressures. In the LJM, with the intermediate-range LJP, both behaviors are observed. The range of the LJP is not sufficient to permit spontaneous DMH without the application of a little pressure.

The healing is rapid, of the order of nanoseconds when rare-gas parameters are used. Void formation is slow, the more so for the shorter-range potential.

Dislocations weaken the shear strength of the monolayer, but even fairly large voids ($\sim$30 atoms) have no dramatic effect on the shear modulus, which seems to be mainly a function of the vacancy concentration.

If we consider the effects of the substrate, the situation becomes more complex. We found that a third degree of freedom favors DMH even in the short-range force system. This may be due to the increased mobility of the vacancies which facilitates the annealing process. In an actual monolayer adsorbed on a substrate, the corrugation in the substrate field may have to be considered. The substrate corrugation does two things: (i) it screens out the interactions between atoms decreasing the effective range of the interparticle interaction and (ii) increases the barrier to diffusion of the vacancies. Therefore, the effects of the substrate modulating field seem to discourage DMH. The high vacancy concentration observed in some rare-gas monolayers adsorbed on graphite indicates significant substrate corrugation effects. The exchange with the gas occurs in a different time scale than the healing of the monolayer and cannot account for the large concentration of vacancies.[28] Structurally these monolayers are therefore quite different from ideal monolayers and are not good candidates for DMH.

It would be interesting to investigate the role that vacancies play in the melting of a physisorbed system in particular one with a weak substrate corrugation, such as Xe on Ag{111}.[29] In an experimental environment thermal vacancies are unavoidable. The vacancies may condense into clusters or they may play a catalytic role in the creation of dislocation dipoles in a form of DMH, producing a melting transition with persistence of bond orientational order as predicted by KTHNY (Ref. 3) theory. The melting transition, from a thermodynamic standpoint, may or may not be continuous.

With respect to the self-healing of damaged two-dimensional systems, such as membranes, our studies suggest that several conditions permit physical mechanisms to be operative: diffusion of the vacancies, a long-range interparticle interaction, and pressure. As we saw above for the PLFM with a third degree of freedom or the 4-8 M, the predominance of one property can diminish the reliance on the others. In biological membranes enough of the above conditions may be satisfied to have physical mechanisms of self-healing. The molecules usually form liquid phases, which presumably implies high diffusion constants.[30] They are embedded in a pressurizing fluid and long-range interactions can be present.

ACKNOWLEDGMENTS

We would like to acknowledge useful discussions with David Boal and Michael Wortis. This work has been supported by the Natural Sciences and Engineering Research Council of Canada and the Office of Naval Research under Contract No. N000140-91-C-0067.

*Electronic address: bjosj@acadvm1.uottawa.ca
†Electronic address: 057220@acadvm1.uottawa.ca
‡Electronic address: duesbery@nrl.navy.mil

[1] P. Dimon, P. M. Horn, M. Sutton, R. J. Birgeneau, and D. E. Moncton, Phys. Rev. B **31**, 437 (1985) (the vacancy concentration at a given point in the phase diagram is obtained by comparing the coverage measured in units of the commensurate $\sqrt{3}\times\sqrt{3}$ density with the expected full coverage calcu-

lated from the lattice constant derived from the structure factor peak); R. J. Birgeneau and M. Sutton (private communication).

[2]B. Joós and M. S. Duesbery, Phys. Rev. Lett. **70**, 2754 (1993); **72**, 3744(E) (1994).

[3]J. M. Kosterlitz and D. J. Thouless, J. Phys. C **6**, 1181 (1973); D. R. Nelson and B. I. Halperin, Phys. Rev. B **19**, 2457 (1979); A. P. Young, *ibid.* **19**, 1855 (1979).

[4]A. J. C. Ladd and W. G. Hoover, Phys. Rev. B **26**, 5469 (1982).

[5]A. J. C. Ladd and W. G. Hoover, J. Chem. Phys. **74**, 1337 (1981).

[6]W. G. Hoover, N. E. Hoover, and W. C. Moss, J. Appl. Phys. **50**, 829 (1979); W. G. Hoover, W. T. Ashurst, and R. J. Olness, J. Chem. Phys. **60**, 4043 (1974); W. G. Hoover, A. J. C. Ladd, and N. E. Hoover, in *Interatomic Potentials and Crystalline Defects,* edited by J. K. Lee (Metallurgical Society, Warrendale, PA, 1981).

[7]F. F. Abraham, Adv. Phys. **35**, 1 (1986).

[8]K. Strandburg, Rev. Mod. Phys. **60**, 161 (198).

[9]J. A. Combs, Phys. Rev. Lett. **61**, 714 (1988); Phys. Rev. B **38**, 6751 (1988).

[10]W. A. Steele, Surf. Sci. **36**, 317 (1973).

[11]H. C. Andersen, J. Chem. Phys. **72**, 2384 (1980).

[12]M. Born and K. Huang, *Dynamical Theory of Crystal Lattices* (Oxford University Press, Oxford, 1954).

[13]A. A. Maradudin, in *Dynamical Properties of Solid,* edited by G. K. Horton and A. A. Maradudin (North-Holland, Amsterdam, 1974), Vol. 1.

[14]D. R. Squire, A. C. Holt, and W. G. Hoover, Physica **42**, 388 (1969).

[15]R. N. Thurston, in *Physical Acoustics,* edited by W. P. Mason (Academic, New York, 1964), Vol. I, Pt. A.

[16]Z. S. Basinski, M. S. Duesbery, A. P. Pogany, R. Taylor, and Y. P. Varshni, Can. J. Phys. **48**, 1480 (1970).

[17]S. Nosé and M. L. Klein, Mol. Phys. **50**, 1055 (1983).

[18]J. R. Ray and A. Rahman, J. Chem. Phys. **80**, 4423 (1984); J. R. Ray, M. C. Moody, and A. Rahman, Phys. Rev. B **33**, 895 (1986).

[19]M. Parrinello and A. Rahman, J. Appl. Phys. **52**, 7182 (1981).

[20]M. Parrinello and A. Rahman, J. Chem. Phys. **76**, 2662 (1982).

[21]M. Sprik, R. W. Impey, and M. L. Klein, Phys. Rev. B **29**, 4368 (1984).

[22]J. R. Ray, M. C. Moody, and A. Rahman, Phys. Rev. B **32**, 733 (1985).

[23]M. S. Duesbery and B. Joós, Philos. Mag. A **54**, 145 (1985) (in Fig. 1 the labels for λ and μ have been inverted).

[24]J. A. Barker, D. Henderson, and F. F. Abraham, Physica **106A**, 226 (1981).

[25]B. Joós and M. S. Duesbery, Phys. Rev. Lett. **55**, 1997 (1985); Phys. Rev. B **33**, 8632 (1986).

[26]B. Grossmann, B. Joós, and M. S. Duesbery, Phys. Rev. B **39**, 7917 (1989).

[27]B. Joós, Q. Ren, and M. S. Duesbery, Surf. Sci. **302**, 385 (1994).

[28]Desorption rates for physisorbed monolayers are of the order of 10^8 s^{-1}. See, for instance, H. J. Kreuzer and Z. W. Gortel, in *Physisorption Kinetics,* edited by G. Ertl and R. Gomer, Springer Series in Surface Sciences Vol. 1 (Springer-Verlag, Berlin, 1986).

[29]N. Greiser, G. A. Held, R. Frahm, R. L. Greene, P. M. Horn, and R. M. Suter, Phys. Rev. Lett. **59**, 1706 (1987), and references therein; A. J. Jin, M. R. Bjurstrom, and M. H. W. Chan, *ibid.* **62**, 1372 (1989).

[30]See, for instance, B. Alberts, D. Bray, J. Lewis, M. Raff, K. Roberts, and J. D. Watson, *Molecular Biology of the Cell,* 2nd ed. (Garland, New York, 1989).